A Shape-Preserving Interpolation: Applications to Semi-Lagrangian Advection

PIOTR HOLNICKI

Systems Research Institute, Polish Academy of Sciences, Warsaw, Poland

(Manuscript received 3 January 1994, in final form 11 July 1994)

ABSTRACT

A high-order interpolation scheme, to be applied in semi-Lagrangian advection algorithms, is discussed. An interpolation polynomial is constructed on a four-point discretization stencil and is then coupled with shape-preserving derivative estimates at the internal mesh points. The obtained interpolate of the advected profile is utilized for integration of a scalar function along the wind trajectories. The discrete maximum principle technique is applied to formulate the positivity conditions of the numerical scheme. Results of computational examples are presented for one- and two-dimensional Lagrangian advection of standard test shapes.

1. Introduction

The main task in computational weather prediction or in modeling the atmospheric transport processes is the finite-dimensional approximation of advection equation. A class of effective and accurate numerical algorithms recently developed for solving the problem is based on the semi-Lagrangian technique (e.g., Bates 1985; Rasch and Williamson 1990; Staniforth and Côté 1991; Smolarkiewicz and Pudykiewicz 1992; Priestley 1993). The numerical scheme in this approach is usually constructed on regular mesh, follows wind field characteristics backward in time, and then employs polynomial interpolation of the initial profile at the upstream departure point. The main advantage of the methods, except numerical convenience of regular mesh discretization, is related to the fact that they admit relatively long time-resolution steps and are therefore computationally very efficient. However, the procedures applied for interpolation of the departure scalar field and defined on a discretization mesh often lead to nonphysical negative values or spurious oscillations, especially in regions of steep gradient. In order that the solution correctly reflects the initial profile suggested by the data, the approximation scheme must be positive definite (monotone if possible) and the numerical diffusion effect should be minimized. Many papers (cf. Fritsch and Butland 1984; Rasch and Williamson 1990; Rančić 1992; Smolarkiewicz and Grell 1992) address this problem and propose techniques to obtain nonoscillatory and shape-preserving solution. In a one-dimensional case, most of the interpolation schemes applied to determine departure profile are based on two consecutive grid points and use either cubic Hermite or rational cubic interpolation, coupled with constrained, shape-preserving estimates of the derivatives at the grid points.

A semi-Lagrangian transport algorithm investigated in the paper is based on the combination of the method of characteristics with a high-degree polynomial interpolation of the departure profile defined on a homogeneous grid. A four-point interpolation stencil is used, with additional shape-preserving constraints imposed on the derivative estimates (Fritsch and Carlson 1980; Fritsch and Butland 1984; Rasch and Williamson 1990) at the internal interpolation points. The scheme considered is still computationally simple, but it enables one to obtain high overall accuracy of the solution due to the fifth-degree interpolation polynomial that can be applied for evaluation of the departure profile. On the other hand, the scheme is relatively compact, which is an advantage for boundary conditions implementation. This is also an important point when local uniform grid refinement is used, since the required grid interfaces are then processed as domain boundaries.

In the next section a general formulation of the interpolation method is presented, and the main relations are derived. Numerical properties of semi-Lagrangian method, coupled with a proposed interpolation algorithm, are considered via characteristics of the amplification factor. The positivity conditions are formulated in section 3 using the discrete maximum principle approach (Ikeda 1983). Shape-preserving properties are related to derivative estimates applied. Results of nu-

Corresponding author address: Dr. Piotr Holnicki, Systems Research Institute, Polish Academy of Sciences, Newelska 6, 01-447, Warsaw, Poland.

merical tests presented in section 4 refer both to one- and two-dimensional cases, where the interpolation scheme is combined with selected implementations of shape-preserving derivative estimates (Rasch and Williamson 1990). They show satisfactory performance for the standard test profiles.

2. Interpolation scheme

Consider a linear advection equation of the form

$$\frac{\partial c}{\partial t} + \mathbf{w}\cdot\nabla c = 0, \tag{2.1}$$

where the scalar quantity $c(x, y, t)$ can represent a concentration of air-polluting factors, and $\mathbf{w}$ is the wind field. The numerical scheme investigated in the sequel refers to one-dimensional (in x direction) constant flow case of (2.1). Moreover, without loss of generality, we can assume $u > 0$ in further analysis.

The computational algorithm considered is related to the upwind semi-Lagrangian approach, where high-degree polynomial interpolation of the initial scalar profile is applied. In order to formally define the approximation scheme, we assume the equidistant spatial discretization with the step h; the time-resolution step will be denoted by τ. The method utilizes the characteristics of a one-dimensional fraction of (2.1) and is based on integrating a profile that arrives at a grid point P at time $(n + 1)\tau$ over the trajectory; that is,

$$c_P^{n+1} = c_*^n, \tag{2.2}$$

where c_*^n is the value of the factor c at the departure point x_* at time $n\tau$.

Construction of the scheme is explained in Fig. 1. The parameter p (an integer number) determines the position of the departure interval in relation to the arrival point P (Bates 1985). It indicates how many intervals upstream from the arrival point lies the interpolation interval. The estimation of c_*^n is obtained as

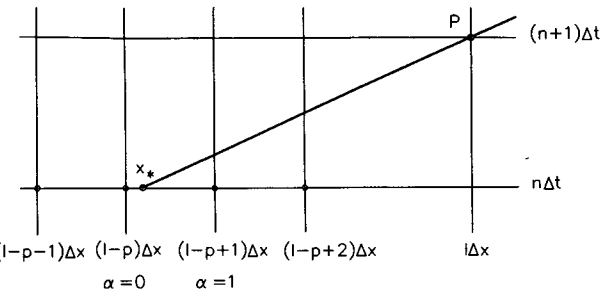

FIG. 1. The four-point interpolation scheme.

polynomial interpolation from four consecutive grid points $x_j = x(I - p + j)$, $(j = -1, \cdots, 2)$.

It is assumed that the interpolant ψ of a given function f in the interval (x_i, x_{i+1}) satisfies the following conditions at interpolation grid points:

$$\psi(x_j) = f_j, \quad \text{for} \quad j = i - 1, \cdots, i + 2,$$

$$\frac{d\psi}{dx}(x_j) = d_j \quad \text{for} \quad j = i, i + 1, \tag{2.3}$$

where we can put $i = I - p$, and d_j are estimates of the derivatives of f at the internal interpolation points. We will assume that the following general constraints are satisfied by the class of the estimates considered:

$$|d_j| \leq \min\{\rho|\Delta_{j-1}|, \rho|\Delta_j|\}, \quad \text{for} \quad \Delta_{j-1}\Delta_j \geq 0,$$

$$d_j = 0, \quad \text{for} \quad \Delta_{j-1}\Delta_j < 0, \tag{2.4}$$

where $\rho > 0$ is a given number, and the discrete slope is defined as $\Delta_j = (f_{j+1} - f_j)/h$.

Let us consider, for notation simplicity, the interval (x_1, x_2). To construct an interpolation polynomial, we can apply a generalized, finite-difference Newton's scheme, which in our case is as follows (without loss of generality we can put $h = 1$):

$$\begin{array}{llllll}
x_0 & f_0 & & & & \\
x_1 & f_1 & \Delta_0 & & & \\
x_1 & — & d_1 & \Delta_{11} & & \\
x_2 & f_2 & \Delta_1 & \Delta_{21} & \tfrac{1}{2}(\Delta_{21} - \Delta_{11}) & \\
x_2 & — & d_2 & \Delta_{22} & \Delta_{22} - \Delta_{21} & \tfrac{1}{4}(2\Delta_{22} - 3\Delta_{21} + \Delta_{11}) \\
x_3 & f_3 & \Delta_2 & \Delta_{32} & \tfrac{1}{2}(\Delta_{32} - \Delta_{22}) & \tfrac{1}{4}(\Delta_{32} - 3\Delta_{22} + 2\Delta_{21}) \quad \tfrac{1}{12}(\Delta_{32} - 5\Delta_{22} + 5\Delta_{21} - \Delta_{11}),
\end{array}$$

where we denote

$$\Delta_{11} = f_0 - f_1 + d_1, \quad \Delta_{21} = -f_1 + f_2 - d_1, \quad \Delta_{22} = f_1 - f_2 + d_2, \quad \Delta_{32} = -f_2 + f_3 - d_2. \tag{2.5}$$

The elements on the diagonal of the above difference diagram constitute the coefficients of the fifth-degree interpolation polynomial. Let us denote (Bates 1985) $\alpha = C - p$, where $C = u\tau/h$, $(0 \leq \alpha \leq 1)$. Thus, it can be easily seen by (2.5) that the interpolation polynomial in the interval (x_1, x_2) has the following form:

$$\varphi(x) = f_0 + (f_1 - f_0)(x - x_0) + [-(f_1 - f_0) + d_1](x - x_0)(x - x_1) + \left[\frac{1}{2}(f_2 - f_0) - d_1\right](x - x_0)(x - x_1)^2 + \left[-\frac{1}{4}(f_2 - f_0) - (f_2 - f_1) + d_1 + \frac{1}{2}d_2\right](x - x_0)(x - x_1)^2(x - x_2) + \left[\frac{1}{12}(f_3 - f_0) + \frac{3}{4}(f_2 - f_1) - \frac{1}{2}(d_1 + d_2)\right](x - x_0)(x - x_1)^2(x - x_2)^2$$

$$= f_0 + (f_1 - f_0)(1 + \alpha) + [-(f_1 - f_0) + d_1]\alpha(1 + \alpha) + \left[\frac{1}{2}(f_2 - f_0) - d_1\right]\alpha^2(1 + \alpha) + \left[-\frac{1}{4}(f_2 - f_0) - (f_2 - f_1) + d_1 + \frac{1}{2}d_2\right]\alpha^2(1 + \alpha)(\alpha - 1) + \left[\frac{1}{12}(f_3 - f_0) + \frac{3}{4}(f_2 - f_1) - \frac{1}{2}(d_1 + d_2)\right]\alpha^2(1 + \alpha)(1 - \alpha)^2. \quad (2.6)$$

By applying interpolation formulas (2.3) and (2.6) to the general relation (2.2), we get the following approximation scheme (boundary conditions are included):

$$c_I^{n+1} = c_{b,I}^{n+1}, \quad (I = 1, \cdots, m),$$

$$c_I^{n+1} = b_{i-1}c_{i-1}^n + b_i c_i^n + b_{i+1}c_{i+1}^n + b_{i+2}c_{i+2}^n + b_i' d_i^n + b_{i+1}' d_{i+1}^n, \quad (I = m + 1, \cdots, k), \quad (2.7)$$

where $i = I - p$ and d_i^n, d_{i+1}^n are characterized by (2.3) and (2.4), and $c_{b,I}^{n+1}$ are the boundary values. It follows from (2.6) that the coefficients in (2.7) are

$$b_{i-1} = \frac{1}{12}\alpha^2(1 - \alpha)^2(2 - \alpha),$$

$$b_i = 1 - \alpha^2\left[1 + (1 - \alpha^2)\left(\frac{7}{4} - \frac{3}{4}\alpha\right)\right],$$

$$b_{i+1} = \frac{1}{4}\alpha^2(1 + \alpha)[2 + (1 - \alpha)(8 - 3\alpha)],$$

$$b_{i+2} = \frac{1}{12}\alpha^2(1 - \alpha^2)(1 - \alpha),$$

$$b_i' = \alpha(1 + \alpha)(1 - \alpha)^2\left(1 - \frac{1}{2}\alpha\right),$$

$$b_{i+1}' = -\frac{1}{2}\alpha^2(1 + \alpha)(1 - \alpha)(2 - \alpha). \quad (2.8)$$

It can be easily verified that for all i ($i = I - p$, $I = m + 1, \cdots, k$),

$$\sum_{l=-1}^{2} b_{i+l} = 1. \quad (2.9)$$

The properties of a numerical method are well characterized by the amplification factor A (Adam 1985; Bates 1985). In the general case of the algorithm (2.7), the frequency characteristics of this factor depend on the slope of the advected profile. Here we consider this relation in the neighborhood of an extremum point, that means—by constraint (2.4)—for $d_i = d_{i+1} = 0$. Assuming a solution in the form

$$c_I^{n+1} = c^n A e^{jlk_\lambda h} = c^0 A^n e^{jlk_\lambda h}, \quad (2.10)$$

we get, by (2.4) and (2.7), the following expression for amplification factor (we denote here $i = I - p$ and $\varphi = k_\lambda h$, where k_λ is the wavenumber):

$$A = [b_i + b_{i-1}e^{-j\varphi} + b_{i+1}e^{j\varphi} + b_{i+2}e^{2j\varphi}]e^{-jp\varphi} = [b_i + (b_{i-1} + b_{i+1})\cos\varphi + b_{i+2}\cos 2\varphi] + j\sin\varphi[(b_{i+1} - b_{i-1}) + 2b_{i+2}\cos\varphi)]e^{-jp\varphi}. \quad (2.11)$$

The modulus and the argument of the amplification factor, by (2.11), are as follows:

$$|A(\varphi)| = \{[b_i + (b_{i-1} + b_{i+1})\cos\varphi + b_{i+2}\cos 2\varphi]^2 + [(b_{i+1} - b_{i-1})\sin\varphi + b_{i+2}\sin 2\varphi]^2\}^{1/2}, \quad (2.12)$$

$$\arg[A(\varphi)] = p\varphi + \tan^{-1}\frac{(b_{i+1} - b_{i-1})\sin\varphi + b_{i+2}\sin 2\varphi}{b_i + (b_{i-1} + b_{i+1})\cos\varphi}. \quad (2.13)$$

It can be easily verified that $|A(\varphi)| \leqslant 1$ for $\alpha \in (0, 1)$; thus the scheme is unconditionally stable.

The modulus (2.12) is plotted in Fig. 2a as a function of wavelength (measured as a number of grid steps) for various α as a parameter. In Fig. 2b, similar plots of $|A(\varphi)|$ versus α are presented for wavelength as a parameter.

It is known (Adam 1985; Bates 1985) that $\lambda = 2h$ is the shortest wavelength that can be resolved by any numerical scheme. The most heavy damping occurs for $\alpha = 0.5$, that is, when the departure point x_* lies in the

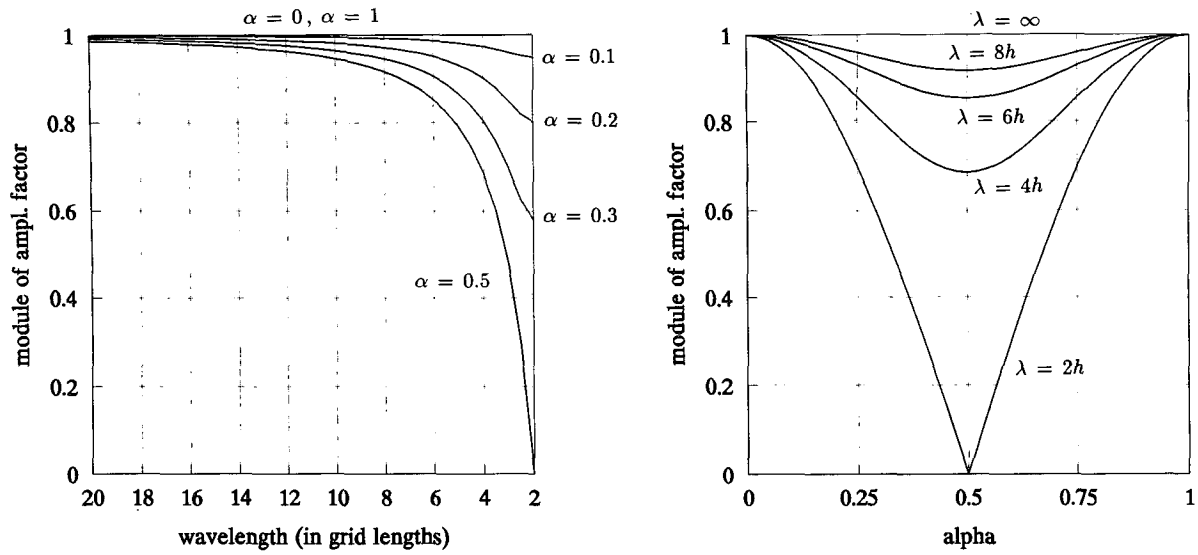

FIG. 2. Modulus of the amplification factor versus (a) wavelength and (b) interpolation parameter α.

center of the interpolation interval. On the other hand, the exact performance is obtained when the departure point coincides with one of the grid points ($\alpha = 0$ or $\alpha = 1$). This fact implies that a substantial increase of accuracy can be obtained by local grid refinement that will depend on the interpolation parameter α.

The relative argument of the amplification factor for the scheme (2.7) (compare Bates 1985) in case $d^n_{I-p} = d^n_{I-p+1} = 0$,

$$\gamma = \frac{\arg[A(\varphi)]}{(p+\alpha)\varphi} = \left[p\varphi + \tan^{-1} \frac{(b_{i+1} - b_{i-1}) \sin\varphi + b_{i+2} \sin 2\varphi}{b_i + (b_{i-1} + b_{i+1}) \cos\varphi} \right] \times \frac{1}{(p+\alpha)\varphi}, \quad (2.14)$$

is plotted in Fig. 3 as a function of wavelength for $\alpha = 0.25$ and for various p as a parameter. One can see that the phase error grows smaller ($\gamma \to 1$) as p increases. This effect is a result of the relatively decreasing influence of interpolation parameters in (2.14) in a case when the advection becomes a dominating factor (it relates to large values of the shift parameter p).

It must be noted that analysis presented in this section assumes that exact coordinates of the departure point of trajectory are available. In practical implementations, this point location is numerically determined by an iterative interpolation procedure (cf. Smolarkiewicz and Pudykiewicz 1992; Smolarkiewicz and Grell 1992) that implies some limiting the time-discretization step.

3. The discrete maximum principle

In this section we formulate the discrete maximum principle for numerical scheme (2.7). This theorem is an analog of a more general, continuous formulation for the advection–diffusion problem. It states that the solution—in case of no internal sources—incurs its extremum values on the boundary or at the initial state. As a consequence, the positivity of the solution is preserved, and over- or undershooting the extremum, nonphysical negative values, and spurious oscillations do

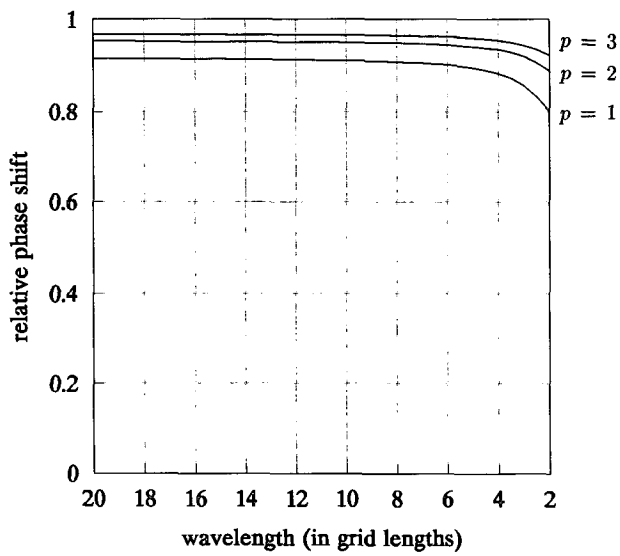

FIG. 3. The relative argument as a function of wavelength.

not appear for nonnegative and respectively smooth initial data.

The technique presented here utilizes Ikeda's (1983) approach; however, some general results formulated there cannot be directly applied because of nonlinear terms related to derivative approximation that appear in (2.7). Some easily seen auxiliary inequalities related to the scheme considered can be formulated as follows.

LEMMA 3.1

The following estimates are satisfied by coefficients (2.8) of the finite-dimensional schemes (2.3), (2.4), and (2.7) for $0 \leqslant \alpha \leqslant 1$ and for all $i = I - p$:

$$\begin{aligned} b_{i-1}, b_i, b_{i+1}, b_{i+2} &\geqslant 0, \\ b'_i &\geqslant 0, \\ b'_{i+1} &\leqslant 0. \end{aligned} \tag{3.1}$$

Moreover, it follows directly from (2.8) that

$$b_i - 2.5b'_i = \frac{1}{2}(\alpha - 1)^3(\alpha^2 - \alpha - 2) \geqslant 0,$$

$$b_{i+1} + 2.5b'_{i+1} = \frac{1}{2}\alpha^3(-\alpha^2 + \alpha + 2) \geqslant 0; \tag{3.2}$$

$$b_i - 3.5b'_i = \frac{1}{2}(\alpha - 1)^2(2\alpha^3 - 3\alpha^2 - 3\alpha + 2) \geqslant -0.0412,$$

$$b_{i+1} + 3.5b'_{i+1} = \frac{1}{2}\alpha^2(-2\alpha^3 + 3\alpha^2 + 3\alpha - 2) \geqslant -0.0412, \tag{3.3}$$

and

$$b_i + b_{i+1} - 3.5(b'_i - b'_{i+1}) = \frac{1}{2}(2\alpha - 1)^2(-\alpha^2 + \alpha + 2) \geqslant 0. \tag{3.4}$$

Now we can formulate the main result concerning the maximum principle for the discrete scheme (2.7).

COROLLARY 3.1

Consider the numerical scheme (2.7), provided the coefficients b_i are defined by (2.8) and the constraint coefficient in (2.4) is $\rho = 2.5$. Then the solution $\bar{c}^{n+1} = (c_1^{n+1}, \cdots, c_k^{n+1})$ satisfies the following maximum principle:

$$\min\Big(\min_{1 \leqslant i \leqslant m} c_{b,I}^{n+1}, \min_{m+1 \leqslant i \leqslant k} c_I^0\Big) \leqslant c_I^{n+1} \leqslant \max\Big(\max_{1 \leqslant i \leqslant m} c_{b,I}^{n+1}, \max_{m+1 \leqslant i \leqslant k} c_I^0\Big). \tag{3.5}$$

PROOF

Let us assume that $c_I^{n+1} = \min_{1 \leqslant j \leqslant m} c_j^{n+1}$. Then the left-hand-side inequality (3.5) holds in the case, where $\min_{m+1 \leqslant j \leqslant k} c_j^{n+1} \leqslant c_I^{n+1}$.

Assume now that $\min_{m+1 \leqslant j \leqslant k} c_j^{n+1} \geqslant c_I^{n+1}$. Then, by definition of (2.7), (2.9), and Lemma 3.1, we have

$$\begin{aligned} c_I^{n+1} &= b_{i-1}c_{i-1}^n + b_i c_i^n + b_{i+1}c_{i+1}^n + b_{i+2}c_{i+2}^n + b'_i d_i^n + b'_{i+1}d_{i+1}^n \\ &\geqslant c_{\min} + b_{i-1}(c_{i-1}^n - c_{\min}) + b_i(c_i^n - c_{\min}) + b_{i+1}(c_{i+1}^n - c_{\min}) + b_{i+2}(c_{i+2}^n - c_{\min}) + b'_i d_i^n + b'_{i+1}d_{i+1}^n \\ &\geqslant c_{\min} + b_{i-1}(c_{i-1}^n - c_{\min}) + b_i(c_i^n - c_{\min}) + b_{i+1}(c_{i+1}^n - c_{\min}) + b_{i+2}(c_{i+2}^n - c_{\min}) \\ &\quad - \rho b'_i \min\{|\Delta_{i-1}|, |\Delta_i|\} + \rho b'_{i+1} \min\{|\Delta_i|, |\Delta_{i+1}|\}. \end{aligned} \tag{3.6}$$

Here and in the sequel we denote $c_{\min} = \min_{m+1 \leqslant j \leqslant k} c_j^{n+1}$ and $c_{\max} = \max_{m+1 \leqslant j \leqslant k} c_j^{n+1}$.

Let $d_i \neq 0$ or $d_{i+1} \neq 0$ [otherwise the left-hand-side inequality (3.5) follows directly from (3.6) and Lemma 3.1]. In the first case we have $c_i^n \neq c_{\min}$, and in the second case $c_i^{n+1} \neq c_{\min}$. Thus, from (3.6), (3.4), and (3.2) we get

$$\begin{aligned} c_I^{n+1} &\geqslant c_{\min} + b_i(c_i^n - c_{\min}) + b_{i+1}(c_{i+1}^n - c_{\min}) - \rho b'_i |c_i^n - c_{i-1}^n| + \rho b'_{i+1}|c_{i+1}^n - c_i^n| \\ &\geqslant c_{\min} + (b_i - \rho b'_i)(c_i^n - c_{\min}) + (b_{i+1} + \rho b'_{i+1})(c_{i+1}^n - c_{\min}) \geqslant c_{\min}. \end{aligned}$$

This completes the proof of the left inequality (3.5). The right-hand-side inequality can be proved similarly.

COROLLARY 3.2

Let the assumptions of Corollary 3.1 hold. If $\rho = 3.5$, then the solution $\bar{c}^{n+1} = (c_1^{n+1}, \cdots, c_k^{n+1})$ satisfies the discrete maximum principle outside local extremum points and can have limited under- or overshootings in vicinity of local extremum.

PROOF

Let us assume that $d_i \neq 0$ and $d_{i+1} \neq 0$ (that means $c_i^n > c_{\min}$ and $c_i^{n+1} > c_{\min}$, respectively). Thus, by

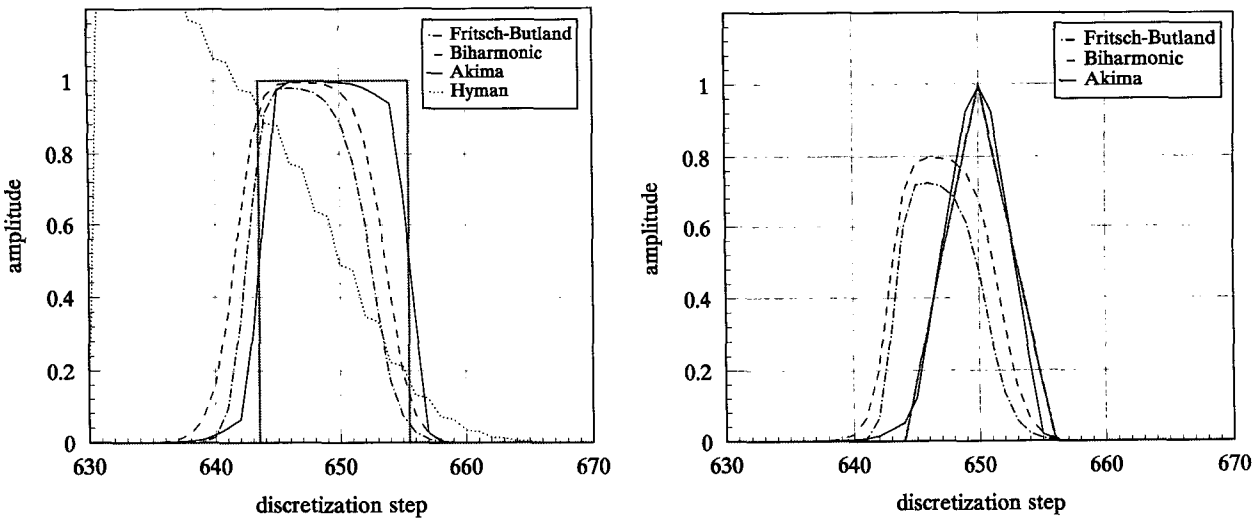

FIG. 4. Advection of the unit amplitude (a) rectangle and (b) triangle profile after 200 time steps.

(3.4), the right-hand-side inequality (3.6) can be estimated in the following form:

$$\begin{aligned} c_I^{n+1} &\geqslant c_{\min} + b_i(c_i^n - c_{\min}) + b_{i+1}(c_{i+1}^n - c_{\min}) \\ &\quad - \rho b_i' \,|\, c_{i+1}^n - c_i^n \,| + \rho b_{i+1}' \,|\, c_{i+1}^n - c_i^n \,| \\ &\geqslant c_{\min} + (b_i + b_{i+1} - \rho b_i' + \rho b_{i+1}')|\Delta_i| \\ &\geqslant c_{\min}. \end{aligned}$$

This implies the left inequality of (3.5), and the right side can be proved in the same way.

In the neighborhood of local minimum we have $c_i^n = c_{\min}$ or $c_i^{n+1} = c_{\min}$, and the left estimate of

$$c_{\min} - 0.0412|\Delta_i| \leqslant c_I^{n+1} \leqslant c_{\max} + 0.0412|\Delta_i|$$

follows from (3.3) and the second inequality (3.6). The right-side estimate can be verified in the same way.

The formulated results state the sufficient conditions of positivity of the scheme considered. Monotonicity properties can be achieved by the respective implementation of the derivative estimate (2.4) coupled with interpolation scheme (2.7). In the next section we present selected numerical results obtained for one-dimensional and two-dimensional advection problems.

4. Numerical results

The test computations discussed in this section have been performed in one-dimensional and two-dimensional cases for several implementations of shape-preserving derivative estimates in the interpolation interval. We consider here the following forms of these estimates, considered previously in Fritsch and Butland (1984), Williamson and Rasch (1989), and Rasch and Williamson (1990):

$$\text{Harmonic mean: } d_j = \begin{cases} \dfrac{2\Delta_{j-1}\Delta_j}{\Delta_{j-1} + \Delta_j}, & \Delta_{j-1}\Delta_j > 0, \\ 0, & \Delta_{j-1}\Delta_j \leqslant 0, \end{cases}$$

Fritsch–Butland:

$$d_j = \begin{cases} \dfrac{3\Delta_{j-1}\Delta_j}{\max(\Delta_{j-1}, \Delta_j) + 2\min(\Delta_{j-1}, \Delta_j)}, \\ \quad \Delta_{j-1}\Delta_j > 0, \\ 0, \ \Delta_{j-1}\Delta_j \leqslant 0, \end{cases}$$

$$\text{Hyman: } d_j = \frac{\Delta_{j-2} - 7\Delta_{j-1} + 7\Delta_j - \Delta_{j+1}}{12},$$

$$\text{Akima: } d_j = \begin{cases} \dfrac{\alpha\Delta_{j-1} + \beta\Delta_j}{\alpha + \beta}, & \alpha + \beta \neq 0, \\ \dfrac{\Delta_{j-1} + \Delta_j}{2}, & \alpha + \beta = 0, \end{cases}$$

where the discrete slope is defined as $\Delta_j = (f_{j+1} - f_j)/h$ and the coefficients in the last formula are $\alpha = |\Delta_{j+1} + \Delta_j|$, $\beta = |\Delta_{j-1} + \Delta_{j-2}|$.

In the one-dimensional case, the test computations were performed for rectangle and triangle initial profiles of the base length $\lambda = 12h$ and for constant advection velocity. The resulting shapes, obtained after 200 time steps, are presented in Fig. 4. They refer to the case of Courant number $C = 3.2$ and illustrate the properties of four derivative estimates listed above. As it can be expected, harmonic and Fritsch–Butland schemes preserve monotonicity, but like other second-order approximates (e.g., arithmetic mean or geometric mean), they degrade the overall accuracy of the method. The resulting solutions are smooth and monotone, but they are "too flat," particularly in the triangle

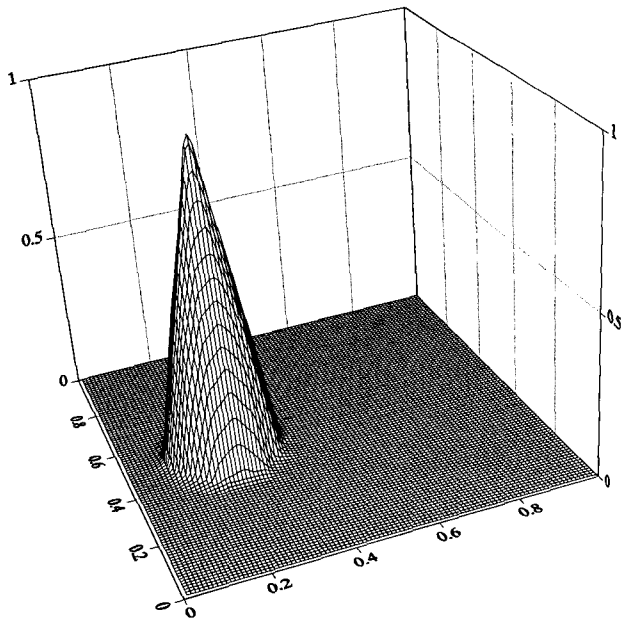

FIG. 5. Rotating cone test ($r_0 = 15h$) after six revolutions.

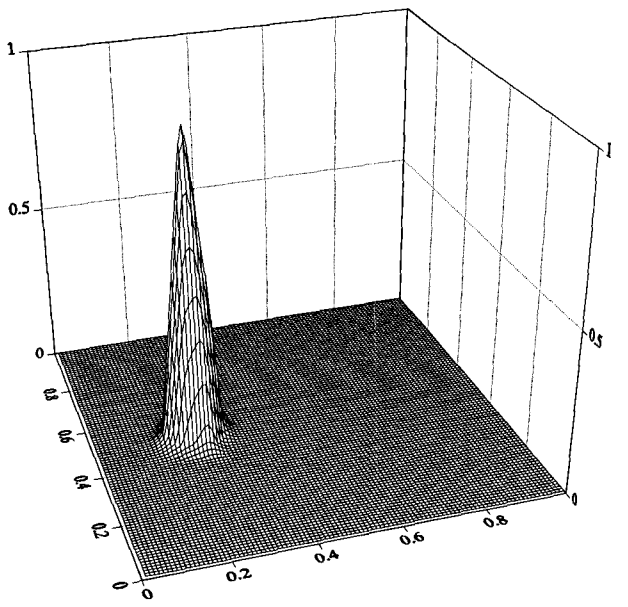

FIG. 6. Rotating cone test ($r_0 = 8h$) after six revolutions.

profile case. The Hyman method, on the other hand, coupled with scheme (2.7), generates unacceptable overshootings and oscillations since it violates the maximum principle conditions (3.1). The higher-order Akima estimate, applied here for the limiter value $\rho = 3.5$ in (2.4), gives remarkably good results in both test shapes.

Two-dimensional examples concern rotating profile cases widely discussed in the literature (cf. Bott 1989; Bermejo and Staniforth 1992; Smolarkiewicz and Grell 1992; Priestley 1992). We consider the square domain $[0, 1] \times [0, 1]$, discretized with a uniform mesh of the step size $h = 0.01$. Tensor product approach is applied to obtain two-dimensional interpolation at a point. Moreover, a two-step iterative procedure is used (see Smolarkiewicz and Pudykiewicz 1992; Smolarkiewicz and Grell 1992) in order to evaluate the departure point's position.

The first test example represents a unit amplitude cone rotating in an advection field of constant angular velocity. The initial profile, placed on the large constant background equal to 25 initial heights of the cone (compare Smolarkiewicz and Grell 1992), is centered at (0.25, 0.5). Two cases of the base radius are considered: (a) $r_0 = 15h$ (or $r_0 = 0.15$) and (b) $r_0 = 8h$. One revolution of the profile is completed in 61 time steps (maximum Courant number is about 7.5). Figures 5 and 6 show the respective resulting profiles after six revolutions, obtained by the scheme (2.7) coupled with Akima-type derivative estimates for the limiting constant in (2.4), $\rho = 3.5$. Good shape-preserving property can be seen in both cases, especially in vicinity of the maximum.

The standard error measures have been used (cf. Takacs 1985) to get some quantitative evaluations of accuracy and to compare numerical results with some other approaches. Given a function f and its approximate solution F calculated on the set of K grid points, the mean-square error is defined as

$$\|f - F\|_h^2 = \frac{1}{K} \sum_k (f_k^n - F_k^n)^2,$$

for the nth time step. It can be shown that the error is a sum of dissipation error and dispersion error

TABLE 1. Error measures for rotating cone test ($r_0 = 15h$).

Time steps	$\int F / \int f_0$	$\int F^2 / \int f_0^2$	max(F)	min(F)	E_{DISS}	E_{DISP}
61	0.9998	0.9996	0.9756	0.0	0.6208E-06	0.3832E-06
122	0.9999	0.9999	0.9769	0.0	0.6326E-06	0.1848E-05
183	1.0001	1.0000	0.9872	0.0	0.6695E-06	0.3553E-05
244	1.0004	0.9999	0.9781	0.0	0.6916E-06	0.5523E-05
305	1.0007	0.9997	0.9712	0.0	0.7017E-06	0.7641E-05
366	1.0010	0.9995	0.9701	0.0	0.7221E-06	0.9882E-05

TABLE 2. Error measures for rotating cone test ($r_0 = 8h$).

Time steps	$\int F/\int f_0$	$\int F^2/\int f_0^2$	max(F)	min(F)	E_{DISS}	E_{DISP}
61	0.9992	0.9980	0.9568	0.0	0.5441E-06	0.1747E-05
122	1.0000	0.9997	0.9632	0.0	0.5647E-06	0.4544E-05
183	1.0020	1.0014	0.9582	0.0	0.5843E-06	0.8097E-05
244	1.0053	1.0043	0.9574	0.0	0.6489E-06	0.1187E-04
305	1.0090	1.0073	0.9628	0.0	0.7292E-06	0.1584E-04
366	1.0118	1.0090	0.9520	0.0	0.7781E-06	0.2065E-04

$$\|f - F\|_h^2 = E_{DISS} + E_{DISP},$$

where

$$E_{DISS} = [\sigma(f) - \sigma(F)]^2 + (\bar{f} - \bar{F})^2,$$

$$E_{DISP} = 2(1 - \rho)\sigma(f)\sigma(F).$$

Here $\bar{f}$ and $\sigma(f)$ denote the mean and the variance, respectively. The correlation coefficient between functions f and F on the set of grid points is denoted by ρ.

Error estimates for two cases of rotating cone experiment are presented in Tables 1 and 2. They can be compared with similar tests considered, for example, by Bott (1989) ($r_0 = 15h$) for flux-corrected transport or by Benjemo and Staniforth (1992) ($r_0 = 8h$) for semi-Lagrangian advection. Generally, the obtained accuracy seems to be satisfactory, and the main relevance of the approach discussed is reated to very low clipping of the cone maximum.

Another two-dimensional computational example concerns rotation of a slotted cylinder (compare Staniforth and Côté 1991; Bermejo and Staniforth 1992; Priestley 1993). The initial profile forms a cylinder with height equal to 4, radius $r_0 = 15h$, and a center at (0.25, 0.5). The slot has the width $6h$ and the length $22h$. The resulting profile, obtained after six revolutions by scheme (2.7) coupled with Akima derivative estimate ($\rho = 3.5$), is shown in Fig. 7.

The computed solution is positive and accurately centered, with no substantial overshootings, and the slot is satisfactory reproduced. Some minor damping the maximum and small shape errors can be seen at the top of the cylinder. On the other hand, the error measures presented in Table 3 are comparable to (or sometimes better than) the similar test results discussed in the literature items quoted before.

5. Conclusions

Numerical efficiency of the method discussed arises from at least two reasons. A general advantage of semi-Lagrangian approach is due to the fact that integration of the advection equations is performed along particle trajectories, so that the solution is more regular and the related approximation error is small. Moreover, the numerical stability conditions are much less restrictive than in Eulerian schemes and are related to departure-point evaluation procedure. As a consequence, a relatively long time-discretization step can be applied. On the other hand, the four-point interpolation scheme employed in (2.7) is computationally simple and provides good approximation of the advected profile (fifth-degree polynomial interpolation).

Computational results presented in the previous section illustrate some properties of interpolation algorithm (2.7) combined with various schemes of derivative approximation. They confirm the general properties of positivity of the scheme formulated in Corollary 3.1 and Corollary 3.2. Monotonicity properties are closely related to the algorithm of derivative estimation, as well as to the specific value of limiting factor ρ in (2.4), which is important near extremum points of the data. These conditions can be automatically preserved by respectively designed schemes, such as arithmetic mean, harmonic mean, and Fritsch–Butland (see Fig. 4). However, the high-degree interpolation polynomial (2.7) is not fully utilized in this case, since the second-order derivative estimates with additional constraint near extremum do degrade the overall accuracy of the method. On the other hand, the high-order schemes (Hyman, Akima) require additional amplitude limits to be imposed on the estimates. The Hyman scheme, however, combined with (2.7), produces

TABLE 3. Error measures for slotted cylinder rotation.

Time steps	$\int F/\int f_0$	$\int F^2/\int f_0^2$	max(F)	min(F)	E_{DISS}	E_{DISP}
61	1.0001	0.8699	3.9974	0.0	4.276E-03	4.319E-02
122	0.9999	0.8529	3.9902	0.0	5.522E-03	4.680E-02
183	0.9997	0.8389	3.9835	0.0	6.678E-03	4.943E-02
244	0.9998	0.8267	3.9774	0.0	7.782E-03	5.198E-02
305	1.0001	0.8159	3.9746	0.0	8.852E-03	5.455E-02
366	1.0005	0.8061	3.9675	0.0	9.848E-03	5.748E-02

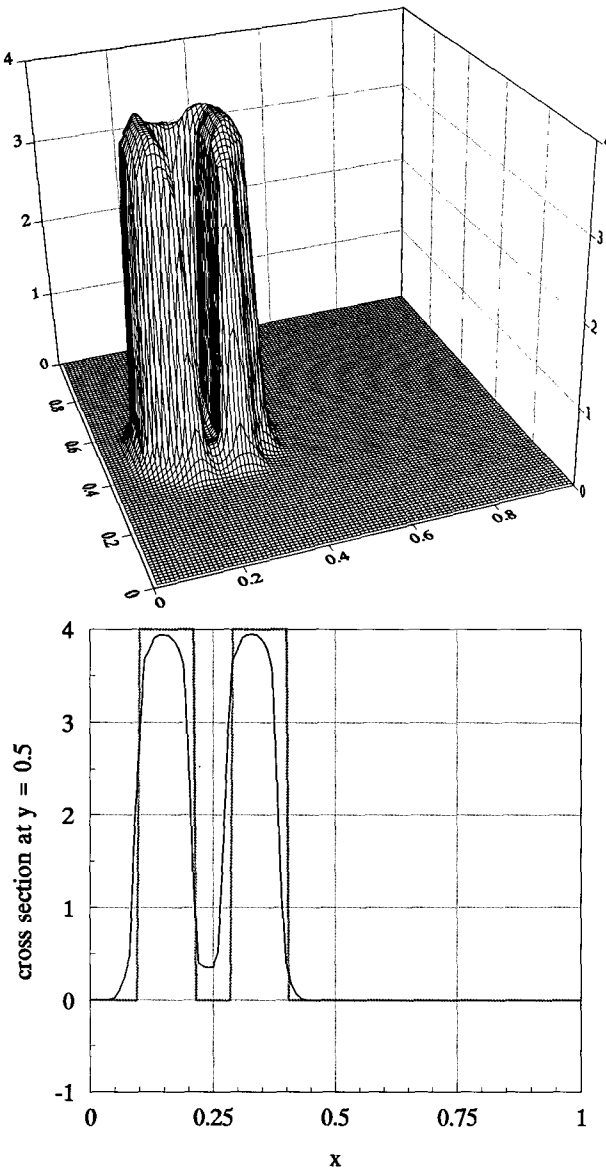

FIG. 7. (a) Slotted cylinder profile after six revolutions and (b) a cross section at $y = 0.5$.

unacceptable oscillations and overshootings for standard test shapes. In this case the maximum principle conditions (3.1) are violated due to the negative components that appear in an explicit way in the main formula of the algorithm. Definitely the best results are given by applying the Akima scheme under some constraint in the neighborhood of the extremum (compare Corollary 3.1 and Corollary 3.2). Here the high order of the derivative estimate can be fully utilized due to fifth-degree interpolation polynomial (2.7). Remarkably good performance of cone and triangle shapes follows from the fact that Akima approach is especially well designed for this type of profiles.

The accuracy of the scheme investigated depends on the position of the departure point in the interpolation interval (see Fig. 2). The method, as other explicit schemes, exactly performs the advected profile in the case when the starting point of the trajectory coincides with the grid node, as for integer Courant number $-C$ ($\alpha = 0$, or $\alpha = 1$). This fact can be used to improve the overall accuracy by local grid refinement (in regions where $\alpha \approx 0.5$).

Generally, the analysis and numerical tests show that the method can be successfully applied in computer models that use a semi-Lagrangian advection technique.

Acknowledgments. Research supported by the Scientific Research Committee (KBN), Grant 06-0467-9101.

REFERENCES

Adam, Y., 1985: Nonlinear instability in advection–diffusion numerical models. *Appl. Math. Model.*, **9,** 434–440.

Bates, J. R., 1985: Semi-Lagrangian advective schemes and their use in meteorological modeling. *Lect. Notes Appl. Math.*, **22,** 1–29.

Bermejo, R., and A. Staniforth, 1992: The conversion of semi-Lagrangian advection schemes to quasi-monotone schemes. *Mon. Wea. Rev.*, **120,** 2622–2632.

Bott, A., 1989: A positive definite scheme obtained by nonlinear renormalization of advection fluxes. *Mon. Wea. Rev.*, **117,** 1006–1015.

Fritsch, F. N., and R. E. Carlson, 1980: Monotone piecewise cubic interpolantion. *SIAM J. Numer. Anal.*, **17,** 238–246.

——, and J. Butland, 1984: A method for constructing local monotone piecewise cubic interpolants. *SIAM J. Sci. Stat. Comput.*, **5,** 300–304.

Ikeda, T., 1983: Maximum principle in models for convection–diffusion phenomena. *Lecture Notes in Applied Mathematics,* Vol. 4, North-Holland, 159 pp.

Priestley, A., 1993: A quasi-conservative version of the semi-Lagrangian advection scheme. *Mon. Wea. Rev.*, **121,** 621–629.

Rančić, M., 1992: Semi-Lagrangian piecewise biparabolic scheme for two-dimensional horizontal advection of a passive scalar. *Mon. Wea. Rev.*, **120,** 1394–1406.

Rasch, P. J., and D. L. Williamson, 1990: On shape-preserving interpolation and semi-Lagrangian transport. *SIAM J. Sci. Stat. Comput.*, **11,** 656–686.

Smolarkiewicz, P., and G. A. Grell, 1992: A class of monotone interpolation schemes. *J. Comput. Phys.*, **101,** 431–440.

——, and J. A. Pudykiewicz, 1992: A class of semi-Lagrangian approximations for fluids. *J. Atmos. Sci.*, **49,** 2082–2096.

Staniforth, A., and J. Côté, 1991: Semi-Lagrangian integration schemes for atmospheric models—A review. *Mon. Wea. Rev.*, **119,** 2206–2223.

Takacs, L. L., 1985: A two-step scheme for the advection equation with minimized dissipation and dispersion errors. *Mon. Wea. Rev.*, **113,** 1050–1065.

Williamson, D. L., and P. J. Rash, 1989: Two-dimensional semi-Lagrangian transport with shape-preserving interpolation. *Mon. Wea. Rev.*, **117,** 102–129.